



**HAL**  
open science

## Fatigue crack detection based on changes of the structure vibration characteristics

Raissa D M Brandão, Nacer Hamzaoui, François Girardin, Pascal Voagner,  
Thierry Mazoyer

► **To cite this version:**

Raissa D M Brandão, Nacer Hamzaoui, François Girardin, Pascal Voagner, Thierry Mazoyer. Fatigue crack detection based on changes of the structure vibration characteristics. *Surveillance* 9, May 2017, Fez (Maroc), Morocco. hal-03983974

**HAL Id: hal-03983974**

**<https://hal.science/hal-03983974>**

Submitted on 11 Feb 2023

**HAL** is a multi-disciplinary open access archive for the deposit and dissemination of scientific research documents, whether they are published or not. The documents may come from teaching and research institutions in France or abroad, or from public or private research centers.

L'archive ouverte pluridisciplinaire **HAL**, est destinée au dépôt et à la diffusion de documents scientifiques de niveau recherche, publiés ou non, émanant des établissements d'enseignement et de recherche français ou étrangers, des laboratoires publics ou privés.

# Fatigue crack detection based on changes of the structure vibration characteristics

Raissa D.M. BRANDÃO<sup>1,2</sup>, Nacer HAMZAOU<sup>1</sup>, François GIRARDIN<sup>1</sup>, Pascal VOAGNER<sup>2</sup>,  
Thierry MAZOYER<sup>2</sup>

<sup>1</sup>Univ Lyon, INSA-Lyon, Laboratoire Vibrations Acoustique  
F-69621 Villeurbanne, France  
{raissa.de-melo-brandao}@insa-lyon.fr

<sup>2</sup>ACOEM Group  
200 Chemin des Ormeaux, 69578 Limonest Cedex, France  
{raissa.demelobrandao}@acoemgroup.com

## Abstract

In order to implement a technique for detecting fatigue cracks in vibrating structures, a test bench was built in the laboratory and an experimental investigation was conducted. The case of this study is a simplistic representation of a bucket wheel excavator from mining industries, designed to have a fragile structural member acting as a mechanical fuse. No artificial excitation is used. The structural member is naturally damaged during operation and its vibration is monitored over time, until the crack occurs. This paper deals with spectral and transmissibility matrices, by means of which two measurements are compared about changes in the frequency content. The emphasis is not on the modal parameters themselves, but on comparing the spectral waveforms by means of two metrics, the relative error and the likelihood metric from a statistical test. The performance of each feature to detect the changes caused by the presence of cracks in the test-bench is illustrated.

## 1 Introduction

Structural health monitoring (SHM) has become a research focus in almost all engineering communities, including the field of mechanical engineering. The reason is clear: the implementation of an effective monitoring strategy increases the industries competitiveness through a better control of the production tools health. The principle consists in periodically evaluating the health state of a machine in order to carry out maintenance operations only at the most convenient time. In this way, SHM encompasses local and global strategies of surveillance [1].

Local SHM methods include visual inspections and non-destructive evaluation techniques, such as acoustic emission, ultrasonic and eddy current. The limitation of all these methods comes from the fact that a priori knowledge of the damage zone location is required. In contrast, global vibration-based methods are an alternative to overcome this limitation and, in some cases, they can be applied with natural excitations. Several works (*e.g.* [1-4]) have made critical reviews on the topic, which has been developed for more than thirty years.

The main idea behind the vibration-based SHM is that damage changes the stiffness, mass and energy dissipation characteristics of the structure and therefore its dynamical behaviour. As stated by Farrar *et al.* [3], the most fundamental challenge of this approach is the fact that damage is typically a local phenomenon and may not significantly influence the lower-frequency global response of a structure that is typically measured during vibration tests. At the same time, it is well-known that environmental factors, such as temperature and moisture, also produce changes in dynamic characteristics [1]. Therefore, making accurate and repeatable vibration measurements at a limited number of locations on structures often operating in adverse environments represents many practical issues [3].

Historically, the vibration-based SHM has been applied to aeronautics, civil structures (bridges and buildings) and offshore platforms. Our objective is to work with industrial machinery submitted to fatigue cracks. We want to implement, from measurement data acquired during operation, a monitoring technique that allows early detection of the presence of cracks that can compromise the correct operation of the machine.

In this way, we have designed an experimental test-bench on the laboratory representing simplified version of a real machine, on which fatigue cracks are naturally generated during operation and its vibration is monitored periodically. The first part of this paper presents the spectral approach developed for monitoring the integrity of structures from its vibration signals. It is based on tracking the frequency content changes on spectral and transmissibility matrices. Then, the experimental setup is detailed and the results obtained are illustrated and discussed.

## 2 Spectral approach for SHM

This section discusses the spectral approach developed in order to detect the existence of structural damage on a machine, through the analysis of its dynamic behaviour. It gives the details on the spectral quantities and their metrics investigated to track the changes on these measured responses.

### 2.1 Spectral and transmissibility functions

Consider a structure subjected to several independent sources of excitation, as illustrated in Figure 1.

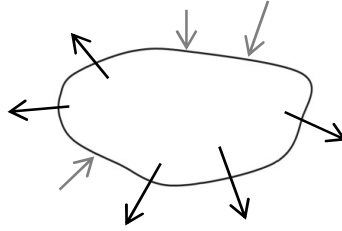


Figure 1: Structure with several inputs (grey arrows) and several measured responses (black arrows).

Let  $x_i(t)$  be the  $i^{\text{th}}$  response signal measured on this structure and  $X_i(f)$  its spectrum at the frequency  $f$ , obtained by a Discrete Fourier Transform (DFT). The spectral matrix  $\mathbf{S}$  is a 3-D matrix that gathers the auto- and cross-spectra functions of the set of  $p$  measured response signals. For a given frequency  $f$ , each element of this matrix is given by the following equation:

$$S_{i,j}(f) = X_i^*(f)X_j(f), \text{ with } i, j = 1, 2, \dots, p \quad (1)$$

where the subscript  $*$  represents the complex conjugate.

The limitation of using spectral matrices in the context of SHM is because they are sensitive to any frequency changes, not only the ones caused by damage. For this reason, the use of transmissibility functions, which do not depend on the excitations as long as the input degrees of freedom do not change, has been extensively investigated. The reader is referred to [5] for a review of literature on the use of transmissibility concept for damage detection and localization.

The transmissibility functions are generally defined as the ratio of the spectra of two homogeneous variables (acceleration response/acceleration input), for a single excitation at a given location [5]. From equation (1), we can define these functions as:

$$T_{i,j}(f) = \frac{S_{i,j}(f)}{S_{i,i}(f)}, \text{ with } i, j = 1, 2, \dots, p \quad (2)$$

However, there are few cases in the practice where only one source of excitation acts on the system of interest. For this reason, the transmissibility concept has been generalized for the case of multiple excitations to a matrix quantity (e.g. see [6]). In this case, under the assumption that the structure behaviour is linear, the  $p$  measured responses and hence the spectral matrix can be split into references and outputs subsets:

$$\mathbf{S}(f) = \begin{bmatrix} \mathbf{S}_{r,r}(f) & \mathbf{S}_{r,o}(f) \\ \mathbf{S}_{o,r}(f) & \mathbf{S}_{o,o}(f) \end{bmatrix} \quad (3)$$

where  $r=1,2,\dots,m$  and  $o=1,2,\dots,(p-m)$  correspond to the  $r^{\text{th}}$  and  $o^{\text{th}}$  measured responses considered respectively as references and output. Therefore, if the number  $m$  of reference responses is at least equal to the number of uncorrelated sources of excitation, the submatrix  $\mathbf{S}_{r,r}(f)$  is well-conditioned and the transmissibility matrix can be defined as [7,8]:

$$\mathbf{T}(f) = \mathbf{S}_{r,o}^T(f) (\mathbf{S}_{r,r}^T(f))^{-1} \quad (4)$$

where the subscript  $^T$  refers to the transpose.

Notice that this definition of the transmissibility matrix is equivalent to the H1 estimator of transfer functions [8]. It represents a linear system that characterises the structure for any excitations applied at the given input degrees of freedom.

## 2.2 Monitoring metrics

With the purpose of determining if a structure is damaged or not, we compare two measurements (at  $t_0$  and at  $t_n > t_0$ ) about changes on the frequency content by means of the estimated spectral and transmissibility matrices.

### 2.2.1 The relative error

The first metric used to monitor the integrity of the structure is based on a relative difference at each frequency of the analysis band. For simplicity, the spectral and transmissibility matrices are generically named here as  $\mathbf{M}(f)$ .

As described in the equation below, it corresponds to the sum of squared absolute errors between the spectral quantities at  $t_k$  and  $t_0$ , normalized by the power of the spectral quantity at  $t_0$ .

$$E_{\mathbf{M}}(f, t_k) = \frac{\sum_j \sum_i \|M_{i,j}^{t_k}(f) - M_{i,j}^{t_0}(f)\|^2}{\sum_j \sum_i \|M_{i,j}^{t_0}(f)\|^2} \quad (5)$$

where the operator  $\|M\|$  represents the complex magnitude of  $M$  and the subscripts  $i$  and  $j$  represents the measured signals composing the matrix  $\mathbf{M}(f)$ .

Thus, the feature used to track the changes is the root-mean-square (RMS) value of  $E_{\mathbf{M}}$ , estimated as:

$$E_{\mathbf{M}}^{\text{RMS}}(t_k) = \sqrt{\frac{1}{n_f} \sum_{f=f_0}^{f_1} (E_{\mathbf{M}}(f, t_k))^2} \quad (6)$$

where  $n_f$  represents the number of frequencies on the analysis band  $[f_0, f_1]$ . In this way, the structure will be considered damaged for large values of  $E_{\mathbf{M}}$  or  $E_{\mathbf{M}}^{\text{RMS}}$ .

### 2.2.2 The likelihood approach

The second metric investigated is based on a hypothesis test.

Let  $\mathbf{x}(t)$  be a  $p$ -variate measured response, such as:

$$\mathbf{x}(t) = [x_1(t) \quad x_2(t) \quad \cdots \quad x_p(t)] \quad (7)$$

Let  $\mathbf{X}(f)$  be the Discrete Fourier Transform (DFT) of the measured response. It derives from the central limit theorem for random variables that the coefficients of the DFT at a given frequency  $f$  will have a complex normal distribution with zero mean and variance equal to the spectral matrix at this particular frequency:

$$\mathbf{X}(f) \sim \mathcal{N}(0, \mathbf{S}(f)) \quad (8)$$

Therefore, the comparison of the measurements at  $t_0$  and  $t_k$  about changes in the frequency content can be seen as a problem of determining if the two measurements come from the same probabilistic distribution. From equation (8), this problem can be encoded in the following hypothesis test:

$$\begin{cases} H_0 & : \mathbf{S}_{t_0}(f) = \mathbf{S}_{t_k}(f), \forall f \\ H_{\text{alternative}} & : \mathbf{S}_{t_0}(f) \neq \mathbf{S}_{t_k}(f), \forall f \end{cases} \quad (9)$$

In other words, if the hypothesis  $H_0$  is accepted, no statistically significant changes occur on the frequency contents of the measurements and, assuming that the measurements points and excitations are the invariant, the system is considered healthy. Alternatively,  $H_0$  is rejected if there are changes on the spectral matrices and, in this case, the system is considered damaged.

The problem described by the equation (9) can be tested by means of the likelihood ratio  $\lambda(f)$ , which is defined by the ratio between the maximum probabilities under each hypothesis. However, when dealing with complex normal distribution, it is interesting to use the negative log-likelihood ratio [9], which is defined in this case as (see Appendix A for more details on this development):

$$\begin{aligned} -\ln \lambda(f) &= N \ln |N^{-1} \mathbf{W}(f)| - n_{t_0} \ln |\mathbf{S}_{t_0}(f)| - n_{t_k} \ln |\mathbf{S}_{t_k}(f)| \\ N &= n_{t_0} + n_{t_k} \\ \mathbf{W}(f) &= n_{t_0} \mathbf{S}_{t_0}(f) - n_{t_k} \mathbf{S}_{t_k}(f) \end{aligned} \quad (10)$$

where  $n_{t_0}$  and  $n_{t_k}$  correspond to the number of averages adopted for the estimation of the spectral matrices at  $t_0$  and  $t_k$  respectively and the operator  $|\mathbf{M}|$  represents the determinant of the matrix  $\mathbf{M}$ . In this way, the hypothesis  $H_0$  is rejected and the structure is considered damaged if this metric reaches a non-negligible value.

For convenience, we have imposed a constant number of averages over the test, such as  $n_{t_0} = n_{t_k} = n$ . In addition, because the determinant of a matrix depends on its dimensions, the statistical metric defined to track changes on the spectral matrices is:

$$V_S(f, t_k) = \frac{-\ln \lambda(f)}{n \cdot p} \quad (11)$$

Here again, the feature used to track the changes over the experimental test is the RMS value of  $V_S$  estimated as in equation (6).

### 3 Experimental setup

The case of study is an experimental test bench representing in a simplistic form a bucket wheel excavator from mining industries (Figure 2). It is composed by a structural member sustaining an electrical motor, the reduction stages and a bucket wheel. The structural member was designed to have a fragile part with exchangeable pieces (two thin plates screwed at positions 1-3 and 2-4), where the crack is expected to appear. The global size of the model is 800 x 240 x 250 mm.

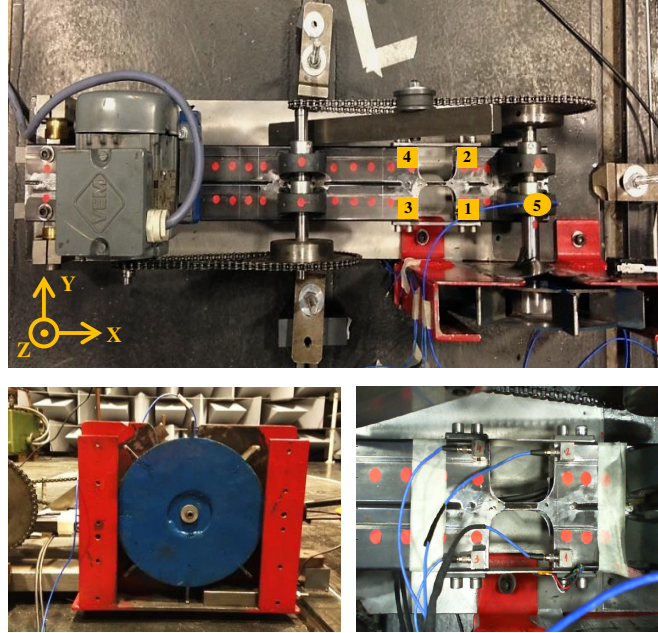


Figure 2: Pictures of the experimental test bench from different points of views.

During the tests, the motor drives the bucket wheel through a step (Figure 2, bottom left), causing shocks. The motor speed (16 Hz), the dimension (20 mm of height) and location (20 mm from the vertical bucket) of the step were chosen to inject enough vibrations on the structure regarding the fatigue damage.

The tests were conducted until the cracks were visually detected (at positions 2 and 3). The vibration of the structural member is monitored periodically (every 5 minutes) in different points by using accelerometers and strain gauges. Table 1 summarizes the sensors position and directions of measurement with respect to the mark point of Figure 2.

Location	Sensors reference
1	$\gamma_1^X, \gamma_1^Y, \gamma_1^Z$
2	$\gamma_2^X, \gamma_2^Y, \gamma_2^Z$
3	$\gamma_3^X, \gamma_3^Y, \gamma_3^Z$ and strain gauges (see Figure 3)
4	$\gamma_4^X, \gamma_4^Y, \gamma_4^Z$
5	$\gamma_5^Z$

Table 1: Sensors location and the respective directions of measurement.

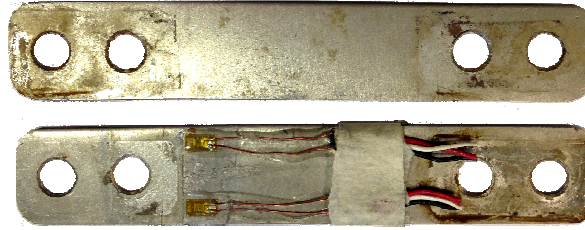


Figure 3: Picture of the exchangeable plates at the end of one test.

It is important to mention that the strain gauges were used to stop the test at a convenient time and, hence, to avoid that other components of the test bench get damaged. They were not used for the SHM spectral approach developed here, because of their frequency limitation. These sensors are based on displacement measurements, so that they cannot measure higher frequencies, which are known to be more sensitive to damaging phenomenon than the lower ones.

Because the vibrations to which the test-bench was subjected were significant and applied to all of its components, other phenomena in addition to the cracks on the exchangeable plates were observed during the tests. For example, it happened that the screws used to fix the motor to the structural member fractured and that the fixation of the test bench to the ground was lost. Because of these other phenomena, some variability was observed between the tests.

The advantage of this experimental strategy is that the fatigue cracks are obtained naturally (i.e. no notch is done a priori). The test bench built in the laboratory is a simplistic representation of the real structure, but allows the investigation of its structural member ageing during operation. In addition to this, no direct measurement of the sources of excitations is done and the analyses are based on response measure only. The perspective is to apply this SHM technique to real complex machines under complex loading conditions, which can also be subjected to varying operational/environmental conditions.

## 4 Application of the SHM spectral approach

The spectral approach presented in this paper was applied to the acceleration signals measured on the experimental test bench. We remind the reader that our objective is to detect, during operation and as soon as possible, the presence of a crack. Therefore, to give the same importance to the changes observed through all frequencies being analysed, the frequency resolution used to the spectral estimates was progressively increased as indicated on Table 2.

Frequency band	Frequency resolution
[0-500] Hz	10 Hz
]500-2000] Hz	20 Hz
]2000 -4000] Hz	50 Hz
]4000-5000] Hz	100 Hz

Table 2: Frequency resolutions used to the spectral estimates.

For the test used as example to demonstrate the results in the following, the crack was visually detected at 85 minutes. At the end of the test – five minutes later, both exchangeable plates were cracked. During this test, it was noticed that one screw, fixing the motor to the structural member, broke. We do not know when exactly it fractured. This screw was changed after the measurement at 55 minutes.

Firstly, the Figure 4 illustrates the relative error metric applied to the spectral matrices estimated during the example test. The thick arrow marks the time when the crack was visually detected.

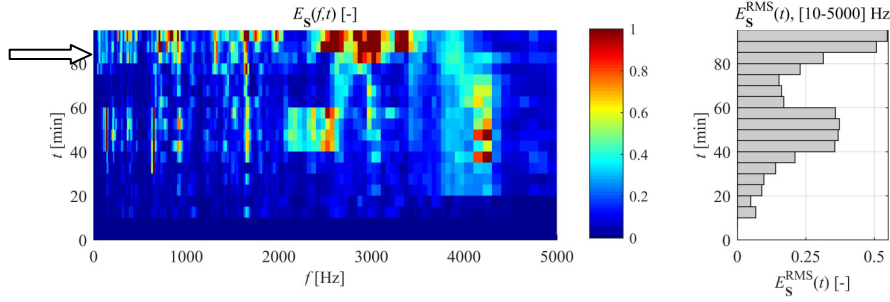


Figure 4: Evolution of the relative error metric for the spectral matrices.

The analysis of the mapping above shows that the most important changes in the spectral matrices occur after 80 or 85 minutes at different frequency bands. An exception is observed between 40 and 55 minutes, but in this case, the changes are probably caused by the problem with the motor screw described before. On the other hand, regarding the RMS value estimated in the frequency band [10-5000] Hz (Figure 4, right), it is clear that the changes detected in the spectral matrices are more significant when they are caused by the presence of the crack. By using this RMS feature to monitor the integrity of the test bench, the detection is possible at the same time as by visual inspection – at 85 minutes.

Secondly, the Figure 5 shows the evolution of the statistical metric during the example test. Once again, the thick arrow marks the time when the crack was visually detected. It is interesting to know that, when this metric reaches the unit value, it means that  $\mathbf{S}_{t_k}(f) \cong 9\mathbf{S}_{t_0}(f)$ . In contrast, when the metric based on the relative error ( $E_S(f,t_k)$ ) has an unit value, then  $\mathbf{S}_{t_k}(f) \cong 2\mathbf{S}_{t_0}(f)$ .

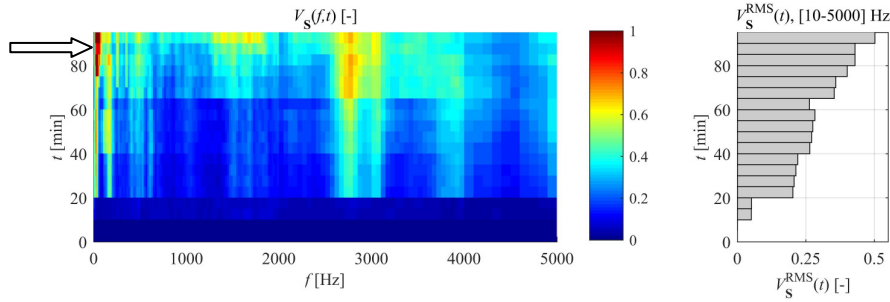


Figure 5: Evolution of the statistical metric for the spectral matrices.

Using this statistical approach, the most significant changes on the spectral matrices are observed in the low frequencies (below to 100 Hz). Also from the analysis Figure 5, this metric seems more robust than the one based on the relative error, considering that the changes between 40 and 55 minutes are no longer detected. In contrast, some less significant changes can be noticed, starting at 20 minutes, for which this metric reaches the value of 0.4 and 0.6 at some frequencies. The RMS value of this metric for the frequency band [10-5000] Hz has an interesting monotonic evolution with ageing, but no abrupt change is clearly noticed near to the time when the crack was visually detected.

It is important to remark that neither of the metrics developed for the spectral matrices circumvents the major limitation of using these quantities in the context of SHM. Frequency changes other than those caused by spectral damage can be detected by these two features. This statement motivated the investigation of the transmissibility matrices.

In this case of study, all measurements being under constant operational conditions, the choice of reference signals was done with respect to the condition number of the submatrix  $\mathbf{S}_{r,r}$ . It is obvious that the mean source of excitation is the rotation of the bucket wheel through the step, so that the signal of the accelerometer placed on the bearing ( $\gamma_5^Z$ ) should be taken as a reference. But only one reference is not sufficient to characterise the excitations sources on the test bench, due to its operational nature. Hence, as a result of an iterative procedure based on the condition number of  $\mathbf{S}_{r,r}$ , the signals retained as references to the transmissibility matrix approach were  $\gamma_2^Y$ ,  $\gamma_3^X$  and  $\gamma_5^Z$ .

The Figure 6 below illustrates the evolution of the relative error metric applied to the transmissibility matrices for the example test.

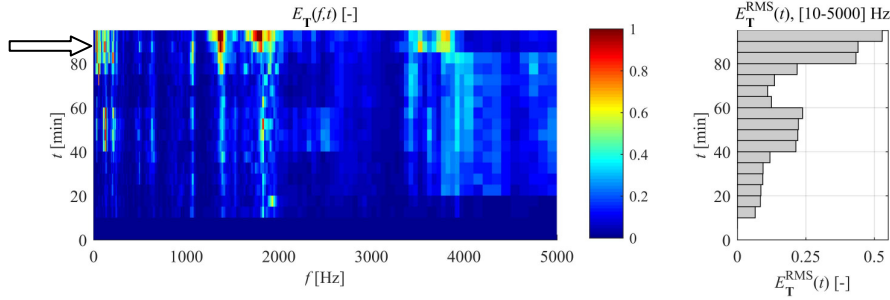


Figure 6: Evolution of the relative error metric for the transmissibility matrices.

The figure above shows important frequency changes starting mainly at 80 or 85 minutes. Notice that the changes between 40 and 55 minutes are also observed in some specific frequencies. Compared to the other metrics, the changes on the  $E_T$  feature are more concentrated to some frequency bands and they seem more stable (the value of this feature is low and approximately constant for most of the example test). Concerning its RMS feature, the evolution observed in Figure 6 (right) is similar to the RMS value of  $E_S$ , and the most important changes observed can be associated with the presence of the crack. By using the transmissibility-based RMS feature instead of the one based on the spectral matrices, the detection can be done five minutes earlier – at 80 minutes.

Finally, to estimate the performance of the features developed to detect the presence of a fatigue crack, the Receiver-Operating-Characteristic (ROC) curve was used. By its definition, the ROC curve shows the trade-off between the true positive rate and false positive rate as one change the threshold for positivity [10]. In this way, if both rates are nearly equals, the detector is considered random, and a good detector will be the one with high true positive rate and small false positive rate.

For our case of study, the true positives were defined from the time when the crack was visually detected. All six tests done with the experimental test-bench were treated together in order to construct a “global-ROC curve” for each of the developed features (Figure 7).

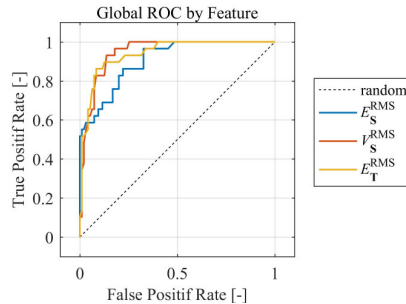


Figure 7: Global ROC curves for each of the developed features.

The figure above demonstrates that the three features developed in this paper have relatively good performances to detect the presence of a crack on the experimental test bench studied. Among them, the worst detection performance is obtained by the RMS  $E_S$  feature. However, even if the performances of the two others are close, the reader should recall that, in contrast to the spectral matrices, the transmissibility matrices are not dependent on the excitations level and type, as long as the input degrees of freedom remain constant.

The ROC curves illustrated in Figure 7 were constructed under constant operational conditions and do not consider the limitation of the use of spectral matrices to SHM. Under varying operational conditions, we expect the performance of the RMS  $E_T$  feature to surpass the others.

## 5 Conclusions

With the purpose of detecting the presence of fatigue cracks in a structure during the machine operation, a spectral approach was developed and its performance tested on an experimental test-bench built in the laboratory. From vibrations measurements on the structure, which can be considered healthy in the beginning of the tests, the idea consisted in tracking changes on spectral and transmissibility matrices, in order to identify the moment when the changes correspond to damage. In this way, a relative error measure and, for the spectral matrices, a statistical metric were investigated.

Even if the statistical metric demonstrated to improve the performance of using the spectral matrices to SHM purposes, both features developed to track changes on these matrices have the limitation of being dependent on the excitation levels. Under varying operational conditions, the best performance is consequently expected for the metric based on the transmissibility matrices. For all experiments performed and for a given threshold, the RMS value of this metric presented a true positive rate of 89.7% and a false positive rate of 12.6%.

The perspective is to apply this SHM technique to real complex machines by taking profit from the statement made by Leclère *et al* [8] that, gathering information from several operational conditions, the transmissibility matrices estimates can be improved through a better characterisation of the structure for given excitation configuration.

## Acknowledgments

This work is supported by the French National Association for Research and Technology (ANRT) and the Brazilian National Council for Scientific and Technological Development (CNPq), under the CIFRE-Brazil program, and performed within the framework of the Labex CeLyA of Université de Lyon, operated by the French National Research Agency (ANR-10-LABX-0060/ ANR-11-IDEX-0007).

## References

- [1] B. Gunes and O. Gunes, *Structural health monitoring and damage assessment - Part I: A critical review of approaches and methods*, Int. J. Phys. Sci., 8(34) (2013), pp. 1694-1702.
- [2] S.W. Doebling, C.R. Farrar, M.B. Prime and D.W. Shevitz, *Damage Identification and Health Monitoring of Structural and Mechanical Systems from Changes in Their Vibration Characteristics: A Literature Review*, Report, Los Alamos National Laboratory, LA-13070-MS, 1996.
- [3] C.R. Farrar, S.W. Doebling and D.A. Nix, *Vibration-based structural damage identification*, Phil. Trans. R. Soc. Lond, A (2001) (359), pp. 131-149.
- [4] C.R. Farrar and K. Worden, *Structural Health Monitoring: a machine learning perspective*, 1<sup>st</sup> edition, John Wiley & Sons, UK, 2013.
- [5] S. Chesné and A. Deraemaeker, *Damage localization using transmissibility functions: A critical review*, Mechanical Systems and Signal Processing, 38 (2013), pp. 569-584.
- [6] A.M.R. Ribeiro, J.M.M. Silva and N.M.M. Maia, *On the generalization of the transmissibility concept*, Mechanical Systems and Signal Processing, 14(1) (2000), pp. 29-35.
- [7] M. Fontul, A.M.R. Ribeiro, J.M.M. Silva and N.M.M. Maia, *Transmissibility matrix in harmonic and random processes*, Shock and Vibration, 11 (2004), pp. 563-571.
- [8] Q. Leclère, N.B. Roozen and C. Sandier, *On the use of the Hs estimator for the experimental assessment of transmissibility matrices*, Mechanical Systems and Signal Processing, 43 (2014), pp. 237-245.
- [9] K.V. Mardia, J.T. Kent and J.M. Bibby, *Multivariate analysis*, 1<sup>st</sup> edition, Academic Press, UK, 1979.
- [10] K. Hajian-Tilaki, *Receiver Operating Characteristic (ROC) Curve Analysis for Medical Diagnostic Test Evaluation*, Caspian J. Intern. Med., 4(2) (2013), pp. 627-635.
- [11] A.A. Miranda, *Spectral Factor Model for Time Series Learning*, PhD Thesis, Université Libre de Bruxelles, Belgium, 2011, Chapter 2, pp.25-40.

## A Appendix

- Likelihood ratio test for spectral densities

The development of the likelihood ratio test for spectral densities presented here is based on the words of Mardia *et al* [9] and Miranda *et al* [11,12].

Suppose  $\mathbf{X}(f)$  be a  $p$ -variate DFT of measured responses. From equation (8), the log-likelihood of observing  $n$  samples of  $\mathbf{X}$  around a target frequency  $f$  becomes (the dependency with  $f$  is omitted):

$$l(\mathbf{X}) = \ln |\pi \mathbf{S}|^{-n} - \sum_{i=1}^n \mathbf{X}_i^* \mathbf{S}^{-1} \mathbf{X}_i \quad (\text{A.1})$$

The likelihood value  $l$  described above represents the probability that  $\mathbf{X}(f)$  follows the complex normal distribution of variance  $\mathbf{S}$  (see equation (8)). Taking advantage of the trace property, this expression becomes:

$$l(\mathbf{X}) = \ln |\pi \mathbf{S}|^{-n} - n \operatorname{tr}(\mathbf{S}^{-1} \Phi) \quad (\text{A.2})$$

$$\Phi = \frac{1}{n} \sum_{i=1}^n \mathbf{X}_i \mathbf{X}_i^*$$

Notice that  $\Phi$  is the sample spectral densities matrix, estimated with  $n$  averages.

Let now  $\mathbf{X}_{t_0} \sim \mathcal{N}(0, \mathbf{S}_{t_0})$  and  $\mathbf{X}_{t_k} \sim \mathcal{N}(0, \mathbf{S}_{t_k})$  be two  $p$ -variate independent measurements, which we want to compare about changes on the frequency content through the hypothesis test defined by equation (9). In this case, the log-likelihood function becomes:

$$l = \ln |\pi \mathbf{S}_{t_0}|^{-n} - n \operatorname{tr}(\mathbf{S}_{t_0}^{-1} \Phi_{t_0}) + \ln |\pi \mathbf{S}_{t_k}|^{-n} - n \operatorname{tr}(\mathbf{S}_{t_k}^{-1} \Phi_{t_k}) \quad (\text{A.3})$$

Under the null hypothesis  $H_0$ ,  $\mathbf{S}_{t_0} = \mathbf{S}_{t_k} = \mathbf{S}$ , so that:

$$l_0 = -Np \ln |\pi| - N \ln |\mathbf{S}| - \operatorname{tr}(\mathbf{S}^{-1} \mathbf{W}) \quad (\text{A.4})$$

$$N = n_{t_0} + n_{t_k}$$

$$\mathbf{W} = n_{t_0} \Phi_{t_0} - n_{t_k} \Phi_{t_k}$$

By consequence, the maximum value that the likelihood function takes under  $H_0$  will be for  $\hat{\mathbf{S}} = N^{-1} \mathbf{W}$ :

$$l_a^{\max} = -Np \ln |\pi| - N \ln |N^{-1} \mathbf{W}| - Np \quad (\text{A.5})$$

On the other hand, under the alternative hypothesis, no constraints are imposed to the expression of the likelihood function and its maximum value will occur for  $\hat{\mathbf{S}}_j = \Phi_j$ :

$$l_a^{\max} = -Np \ln |\pi| - (n_{t_0} \ln |\Phi_{t_0}| + n_{t_k} \ln |\Phi_{t_k}|) - Np \quad (\text{A.6})$$

As a result, the hypothesis test from equation (9) can be tested using the following metric:

$$-\ln \lambda = (l_a^{\max} - l_0^{\max}) = -Np \ln |N^{-1} \mathbf{W}| - n_{t_0} \ln |\Phi_{t_0}| - n_{t_k} \ln |\Phi_{t_k}| \quad (\text{A.7})$$

That means,  $H_0$  is rejected if  $-\ln \lambda \gg 0, \forall f$  (the reader should recall that the dependency with frequency was omitted for simplicity).

It is important emphasize that  $\Phi$  corresponds to an estimate of the spectral matrix, so that the equation (A.7) is equivalent to the equation to the equation (10) presented earlier in this paper.